RESEARCH PAPER
Contrib. Sci. & Tech Eng, 2024, 1(2)
Homepage: https://cste.journals.umz.ac.ir/
DOI: 10.22080/cste.2024.5092

The Effect of Field Intensity on Magnetic Nanoparticles in The Conical Neck of Abdominal Aortic Vessel: Numerical Simulation

Shabnam Shahri [1], Mohsen Pourfallah [2,3]*, Mosayeb Gholinia [1]

[1] *Babol Noshirvani University of Technology, Babol, Iran.*

[2] *Mazandaran University of Science and Technology, Babol, Iran.*

[3] *Mechanical Engineering Department, Tennessee Tech University, Cookeville, United States.*

Article Info
Received 8 April 2024
Accepted 14 May 2024
Available online 1 June 2024

Keywords:
Drug Delivery;
Magnetic Nanoparticles;
Fe_3O_4;
MHD;
Abdominal Aortic Aneurysm.

Abstract:
In the current era of the availability of computational fluid dynamics tools and high-performance computers, it is possible to simulate complex physical phenomena within the human body. One of the most studied areas of this field is drug delivery. Drug path control is one of the processes that can greatly help many diseases. Using the new drug delivery system, also called "controlled release drug delivery system", three domains of speed, time, and place of drug release can be controlled, resulting in minimizing unwanted side effects on other vital tissues, which leads to lower drug doses. This study aims to investigate the transfer of Fe3O4 nanoparticles in the presence of a magnetic field in a three-dimensional model of the Angulated Neck of Abdominal Aortic Aneurysm (AAA) extracted from the literature. The ideal aortic model includes the proximal angular neck, the aneurysm sac, and the iliac arteries. Uniform nanoparticles in a specific position relative to the angled neck of the aorta are modeled with the k - ω turbulence model. The Euler- Lagrangian (E-L) approach and the magnetic hydrodynamic model (MHD) in the ANSYS solution are targeted to investigate TD nanoparticles. These nanoparticles are tracked at two different magnetic field positions located near the abdominal aorta and examined by applying different magnetic numbers.

***Corresponding Author:** mpourfall42@tntech.edu

Supplementary information: Supplementary information for this article is available at https://cste.journals.umz.ac.ir/

Please cite this paper as: Shahri, S., Pourfallah, M., &, Gholinia, M. (2024). The Effect of Field Intensity on Magnetic Nanoparticles in The Conical Neck of Abdominal Aortic Vessel: Numerical Simulation. Contributions of Science and Technology for Engineering, 1(2), 19-28. doi:10.22080/cste.2024.5092.

1. Introduction

Intravenous blood flow, intercellular fluid behavior, fluid behavior within various vital organs, etc., are examples of countless instances of fluid movement within living tissues. The analysis of blood flow in the arteries is one area of communication between medical science and mechanics. In fluid mechanics, blood is considered to be a non-Newtonian material, and its viscosity changes with the applied strain rate. However, it is sometimes considered according to the conditions of the problem, the desired organ, and the ease of the Newtonian solution process. According to Guyton and Hall's Textbook, the physical behavior of blood in various organs of the body is different [1-4]. One of the newest techniques in modern drug delivery, which has received much attention in recent years, both from the medical and mechanical engineering communities, due to the considerably reduced negative effects of drugs on healthy tissues, is the transfer of drugs using magnetic nanoparticles. Due to controlling and slowing the release of the drug, protection of the drug molecule, the smaller particle size of the cell, the ability to cross biological barriers to deliver the drug to the target site, increased drug retention time, targeted drug delivery, and biocompatibility. These structures can be considered a very effective drug delivery system, which increases the therapeutic efficacy of the drug [5-7]. Iron oxide superparamagnetic nanoparticles are another important and widely used class of inorganic materials used in drug delivery. They can be prepared using chemical methods such as co-precipitation or biological methods using bacteria that have superparamagnetic properties, allowing these compounds to be used in targeted drug delivery using a magnetic field [8, 9]. Drug delivery using nanocarriers due to pharmacokinetic changes of the drug, increasing the presence of the drug in the bloodstream, reducing toxicity, increasing the half-life of the drug, reducing the systematic drug distribution, reducing drug use, and more accurate targeting is considered as one of the promising solutions in the treatment of cancer and incurable diseases. Based on the abovementioned reasons, the efficiency of magnetic nanoparticles in this field will be more significant [10, 11]. One of the best advantages of

*ISSN **3060-6578***

these particles is the ability to control their movement by applying an external magnetic field to the particles [12, 13]. Regarding the valuable assistance of mechanical engineering in the field of CFD simulations of targeted transfer of nanoparticles with the presence of a magnetic field, we have seen the facilitation of the upward trend in this field. The main subject of this paper is the study of drug transfer by magnetic nanoparticles by Fe_3O_4 nanoparticles in the presence of an external field, in which much research has been done. For example, the research conducted by Hoshiar et al, 2017 [14] considered the accumulation of nanoparticles, and despite the potential and promising results of nanoparticles, this accumulation prevents the precise conduction of particles in the arteries. Lim et al., 2019 [15] examined Fe_3O_4 nanoparticles in an in vivo experiment. The magnetic field was used on mice, and the nanomagnetic particles were placed in the myocardium and the absorption of these particles, in this case, was higher than in the experiment without the magnetic field. Salem and Tuchin, 2020 [16] considered the blood biomagnetic fluid to be incompressible and magnetic, simulated it in a rectangular tube, and applied the field by a permanent magnet outside the tube. The results of this study can be used in many biomedical applications, such as the use of magnetic nanoparticles in drug delivery and targeting. To evaluate drug delivery, distribution, and drug persistence, Jafarzadeh et al, 2020 [17] simulated an abdominal aortic aneurysm. The blood fluid enters as a non-Newtonian input fluid that depends on hematocrit and pressure, and magnetic particles carrying iron oxide are injected into the arteries during a cardiac cycle. The results were evaluated in different hematocrits, and it was observed that hematocrit significantly affects drug duration or retention time. Sodagar et al, 2020 [18] simulated the method of magnetic drug delivery using a magnetic field based on the effect of parameters such as non-Newtonian viscosity, oscillating input, motion, and the presence of atherosclerosis. Their study examined a 90-degree bend in three phases, including no atherosclerosis, moderate atherosclerosis (45%), and severe atherosclerosis (75%), in both fixed and mobile arteries due to expansion and contraction of the heart. The results in these phases of atherosclerosis showed that the presence of atherosclerosis increases the percentage of particle uptake. The effect of mixing and dispersing a fluid drug using computational fluid dynamics (CFD) in a coronary artery model was analyzed by Sarker et al, 2020 [5]. The parameters of this study are used to build custom prototypes for in vivo experiments. Zhang et al, 2020 [6] examined the method of drug-carrying nanoparticles for a specific atherosclerotic patient in the presence of an external magnetic field using the Eulerian-Lagrangian. In this paper, plaques and vascular walls are introduced as a porous medium reported by the Darcy-Forcheimer model in targeted drug delivery. The results show that the particle transfer efficiency depends on atherosclerosis and the characteristics of the external magnetic field, such as position and intensity. According to the studies, it is clear that targeted drug delivery with metal nanoparticles using magnetic current is an ideal and desirable technique that can be used in certain diseases.

This study aims to provide an external magnetic field for the development of future therapies and to provide an understanding of the transfer and deposition of nanomagnetic particles in the target area. In this paper, modeling and simulation of uniform nanoparticle transport and deposition in the specific position of the Angulated Neck of Abdominal Aortic Aneurysm (AAA) is performed by the chaotic simulation method of the low Reynolds number k - ω model. The Euler-Lagrangian (E-L) approach and the magnetic hydrodynamic model (MHD) in ANSYS fluid solution are targeted to investigate the transfer and deposition of nanoparticles. The aerosol drug particles are directed to the target position under external magnetic force and applied to two different angulated neck of abdominal aortic aneurysm (AAA). Aneurysm is an abnormal local enlargement of a part of a blood vessel. This morphological abnormality occurs when the aortic wall becomes vulnerable and weak. In general, due to the importance of the disease and the fact that no research has been done in this field, a numerical particle tracking model has been developed to predict the targeting behavior of magnetic drugs in the Angulated Neck of Abdominal Aortic Aneurysm. Numerical results indicate that the intensity of the magnetic field applied to the deposition efficiency of nanoparticles in two different magnetic field positions, as well as the effect of the field on the retention time of drug-carrying particles, are different, which can be useful for targeted drug delivery to a specific area of the abdominal aorta after extensive clinical trials. This procedure will also be cost-effective and minimize unwanted side effects due to the systematic distribution of the drug in the aneurysm area.

2. Model Description

2.1. Geometry and Boundary Conditions

In this study, a three-dimensional model of the angular neck of the abdominal aorta extracted from the literature was used, and the ideal aortic model includes the proximal or primary angular necks, the aneurysm sac, and the iliac arteries. Also, in this study, to provide an external magnetic field for the development of future therapies, an understanding of nanomagnetic particles in the region of interest is presented. Uniform nanoparticles are modeled in a specific position from the angled neck of the aorta using $k-\omega$ turbulence model. The Euler-Lagrangian (E-L) approach and the magnetic hydrodynamic model (MHD) in the ANSYS solution are considered for the investigation of TD nanoparticles. These nanoparticles were detected at two different magnetic field positions near the abdominal aorta.

The geometry used in this study is modeled using Catia software. The construction of this geometry is similar to the shape of the angulated neck of AAA, shown in **Error! Reference source not found.**. The largest part of the aortic vein is located in the abdominal area of the body (from the diaphragm to the waist (abdominal cavity)). As part of the aorta, the abdominal aorta is essentially a large continuation of the descending aorta located in the thoracic region. The geometry with 20 mm inlet, 55 mm aneurysm sac, and 11 mm and 10 mm for outlet iliac vessels, as well as the selected lengths and six plates with black lines (A-F), are shown in **Error! Reference source not found.**. A and B are

in the upper part of the neck, C is in the middle sac, and D to F are in the iliac branch. A proximal neck angle of 80 ° was chosen, indicating a severe angle of the abdominal aortic neck. This is based on the work reported by Hobo et al. [19], which states a proximal neck angle greater than 60 ° is considered dangerous for endovascular repair.

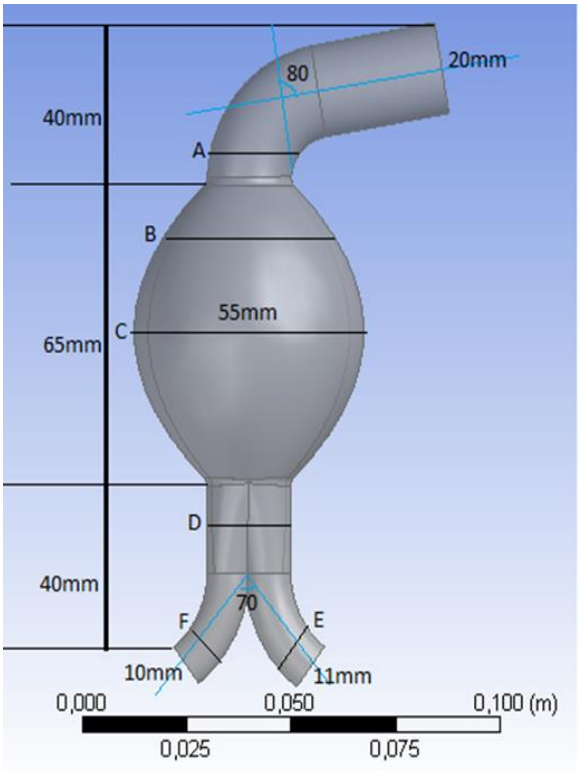

Figure 1. Three-dimensional model of the An Angulated Neck of an ideal AAA

The fluid entering the blood has a density of 1,060 kg/m^3, non-Newtonian and magnetic nanoparticles, and is iron oxide (Fe_3O_4). The characteristics of Fe_3O_4 nanoparticles are shown in **Error! Reference source not found.** [20]. Fixed wall conditions were considered, and for boundary conditions, wall conditions were considered as trap and conducting for the target position. The output condition was considered as a pressure output and omega values, and for the input condition, a uniform mass flow was applied. For pulsed simulation, a user-defined code (UDF) was applied to the time-dependent speed at the input boundary. The waveform obtained from Algebra et al. [21] is used for an abdominal aortic region. The arterial wall, in both cases, acts as a rigid and non-slip condition.

Table 1. Characteristics of magnetic nanoparticles Fe_3O_4

Variable	Value
Nanoparticle density	5100 kg/m^3
Nanoparticle magnetic sensitivity	2.1

2.2. Mathematica Equation

The three-dimensional finite volume method was employed to solve the Navier-Stokes continuity and momentum equations [22] for incompressible and Newtonian fluids. The governing equations for the continuity and motion are as follows:

$$\frac{\partial u_i}{\partial x_i} = 0 \quad (1)$$

$$\frac{\partial u_i}{\partial t} + \partial_j \frac{\partial u_i}{\partial x_j} = -\frac{1}{\rho_f}\frac{\partial p}{\partial x_i} + \frac{\partial}{\partial x_i}\left[\left(\upsilon_f + \upsilon_t\right)\left(\frac{\partial u_i}{\partial x_j} + \frac{\partial u_j}{\partial x_i}\right)\right] \quad (2)$$

In this problem, the turbulent model $k-\omega$, which is a two-equation model, was used. Two-equation models can be considered as the basis of many studies in the field of turbulence flows. The $k-\omega$ model, while simple, adapts well to experimental results, leading to its use in most simulations in the field of mechanical engineering [22, 23]. This model is calculated for numerical simulations with a maximum Reynolds number of 5×10^{-3}. The $k-\omega$ governing equations are written as follows [22]:

$$\frac{\partial k}{\partial t} + u_j \frac{\partial k}{\partial x_i} = p - \beta^*\omega k + \frac{\partial}{\partial x_i}\left[\left(\upsilon_f + \alpha_k\alpha^*\frac{k}{\omega}\right)\frac{\partial k}{\partial x_i}\right] \quad (3)$$

For the pseudo vorticity equation, we have:

$$\frac{\partial \omega}{\partial t} + u_j \frac{\partial \omega}{\partial x_i} = \frac{\gamma\omega}{k}P - \beta\omega^2 + \frac{\partial}{\partial x_i}\frac{\alpha_d}{\omega}\frac{\partial k}{\partial x_i}\frac{\partial \omega}{\partial x_i} \quad (4)$$

$$P = \tau_{ij}\frac{\partial u_i}{\partial x_j}, \tau_{ij} = \nu t\left(2S_{ij} - \frac{2}{3}\frac{\partial u_k}{\partial x_k}, \delta_{ij}\right) - \frac{2}{3}k\delta_{ij}, \delta_{ij} = \frac{1}{2}\left(\frac{\partial u_i}{\partial x_j} + \frac{\partial u_j}{\partial x_i}\right), \beta = \beta_0 f_\beta \quad (5)$$

Thus, according to the above equations, the turbulence viscosity υ_T is as follows [24]:

$$\upsilon_T = C_\mu f_\mu \frac{k}{\omega} \quad (6)$$

$$f_u = exp\left[-\frac{3.4}{\left(1+\frac{R_T}{50}\right)^2}\right], R_T = \frac{\rho K}{(\mu\omega)} \quad (7)$$

The other values of the coefficients used in the above equation are as follows [22]:

$$R_\beta = 8, R_\omega = 2.95, R_K = 6, \alpha_0 = \frac{1}{9},$$
$$\beta_0 = 0.0708, \beta^*{}_0 = 0.09, \alpha^*{}_0 = 1, \sigma_W = \alpha_K = 0.5$$

In this analysis, the deposition efficiency (DE) is the ratio of trapped particles to the total injected particles, which is determined by calculating the percentage of trapped particles as follows [25]:

$$DE = \frac{Deposited\ particle\ number\ in\ the\ specific\ position}{Total\ number\ of\ injected\ particle} \times 100 \quad (8)$$

Particle tracking methods are usually based on the Eulerian-Lagrangian method. Fluid flow in these methods is dissolved on a fixed lattice, and particles that are smaller than the lattice size are followed by Lagrangian. These methods are commonly referred to as discrete particle models or other discrete component models. In these methods, the interaction of particle-fluid, particle-wall, particle-particle, and fluid-particle can be considered.

In this model, the Lagrangian particle tracking scheme and the solution based on finite volume ANSYS-Fluent with Euler-Lagrangian (E-L) [26] approach and magneto-hydrodynamic model (MHD) have been used to investigate

TD particles of abdominal aortic aneurysm. Euler-Euler and Euler-Lagrange (E-L) approaches are commonly used to simulate nanoparticles. The E-L method solves the particle path equation, while the E-E method is used to solve the convective diffusion equations. The E-L method tracks the path of individual particles by considering inertia, electrostatic effects, penetration rate, and wall proximity. The present study uses the E-L method because nanoparticles are less than 100 nm [27]. In the Eulerian-Lagrangian method, the force balance equation for single particles is given as follows:

$$\vec{F} = \overrightarrow{F_D} + \overrightarrow{F_M} = m_p . \frac{d\overrightarrow{U_P}}{dt} \quad (9)$$

where U_p is the velocity of the particles and F is the force. F_D and F_M are drag and magnetic forces, respectively. Brownian motion is intended to simulate nanoparticles. A suitable particle motion equation for calculating single particles has been solved.

$$\frac{du_p^i}{dt} = F_D\left(u_i^g - u_i^p\right) + F_{Brownian} + F_{Lift} + \frac{\rho_p - \rho_g}{\rho_p} g_i \quad (10)$$

For a spherical particle, the Stokes-Cunningham tensile force is expressed as follows:

$$\overrightarrow{F_D} = \frac{18\mu g}{\rho_p {d_p}^2 C_c} \quad (11)$$

$$C_c = 1 + \frac{2\lambda}{d_p}\left(1.257 + 0.4e^{-1.1\frac{d_p}{2\lambda}}\right) \quad (12)$$

where C_c is the Cunningham correction coefficient. Specific correction coefficient values are used for particles of different diameters. Here ρ_p and d_p are the particle density and particle diameter, respectively, and λ is the mean free path of the gas molecules. The Brownian force amplitude is also defined as follows:

$$F_{Brownian} = \xi \sqrt{\frac{\pi s_0}{\Delta t}} \quad (13)$$

where ξ stands for the unit of variance of the independent Gaussian random number, Δt is the particle step time integration, and s_0 is the spectral intensity.

The magnetic force of the present study, FM, is calculated as follows:

$$\overrightarrow{F_M} = \frac{1}{2}\mu_0 x V_P \nabla\left(\overrightarrow{H^2}\right) \quad (14)$$

In the above equation, μ_0 represents the magnetic permeability, x is the magnetic sensitivity of the particle, V_P is the volume of the particle and H is the magnetic field strength. Particle magnetic sensitivity is defined as follows [22]:

$$x = -0.14 d_p . 10^6 + 0.9 \quad (15)$$

where d_p is the particle diameter. The magnetic number Mn (in Tesla) is defined as follows [22]:

$$M_n = \mu_0 H_0 \quad (16)$$

H_0 is the strength of the characteristic magnetic field. The magnetic number depends on the strength of the magnetic field. In this analysis, a comparison of TD nanoparticle particles in two different target positions for magnetic numbers 0.2, 1.6, and 2.8 and particle diameters of 1, 50, 100, and 500 nm has been performed to obtain the desired result.

2.3. Mesh Independency Analysis

Error! Reference source not found. shows an example of a configuration of the computational domain used in the study. To obtain the minimum size of a cell, the grid independence study is considered. The maximum pressure obtained from the five mesh simulations is presented in Figure 3. The diagram shows that with increasing the elements up to 500000, the maximum pressure element decreases, and then with increasing the elements, the maximum pressure increases and converges after $1.5 \times 10^{+6}$. A similar velocity trend was observed for case 4 (972, 832 elements) and case 5 (1, 029, 702 elements). Therefore, in this computational study, a case with 972,832 elements were used.

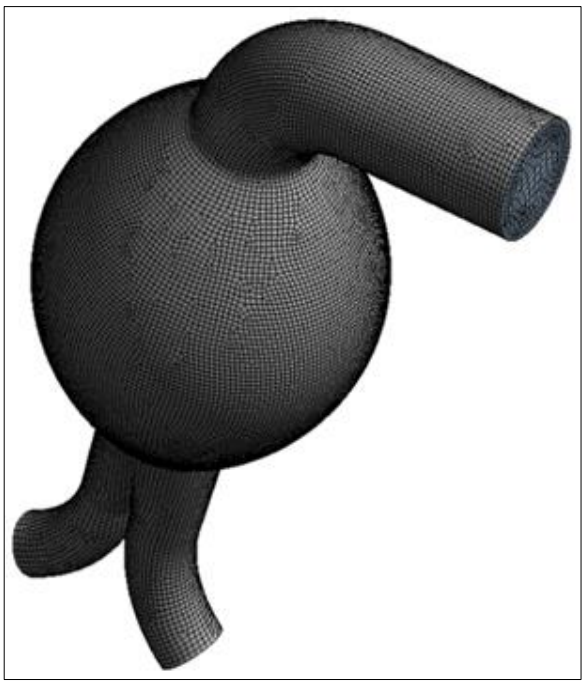

Figure 2. A view of the meshing of the present problem

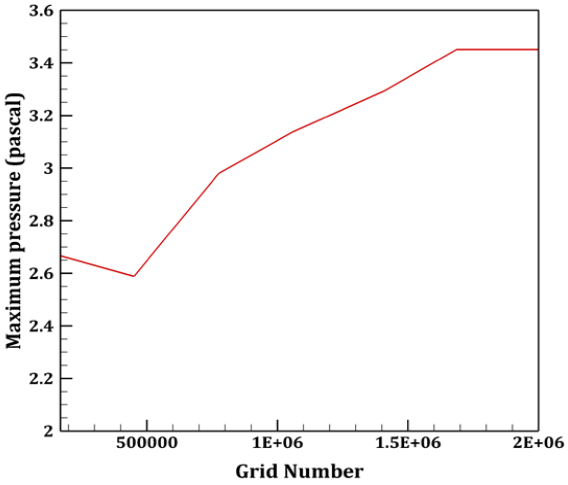

Figure 3. **Maximum pressure grid convergence**

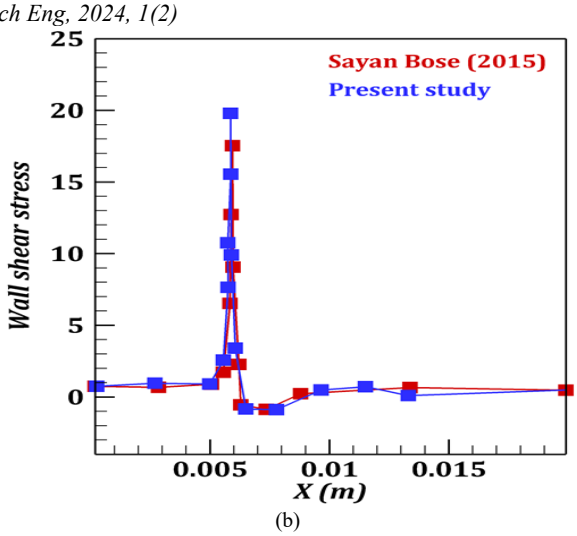

(b)

Figure 4. **a) Comparison of input parabolic velocity of Algabri et al. [21] and the present study, b) Comparison of input wall shear stress of Bose et al. [28] and the present**

2.4. Validation

A comprehensive validation has been performed for the present numerical study. A comparison of the simulation results of magnetic nanoparticle transfer in the presence of the field with the results of Algabri et al [21] was performed. According to **Error! Reference source not found.**-a, the results verified the accuracy of the UDF employed in this study. Also, the results of the simulation of magnetic nanoparticle transfer without the presence of a magnetic field in a two-dimensional plug vessel with Reynolds number 100 for the WSS vessel wall shear stress diagram were evaluated versus the results obtained by Bose et al. [28]. As can be seen in **Error! Reference source not found.**-b, a negative value in WSS means that the zone with low WSS and flow becomes separated. The present numerical results indicate a well-matched trend throughout the length of the blood vessel.

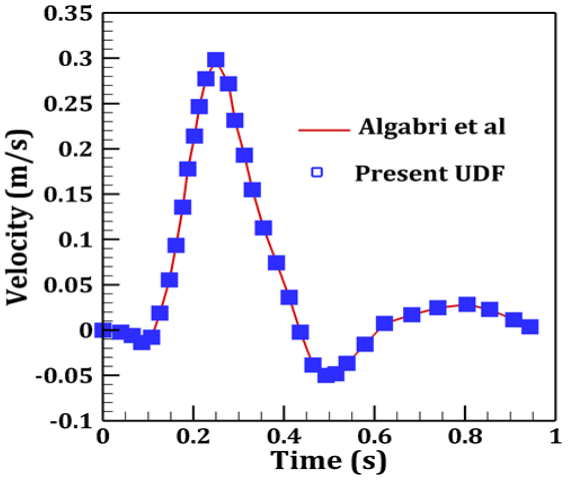

(a)

3. Results and Discussion

The conical neck model of the present abdominal aortic aneurysm is designed to calculate the effect of magnetic number or the same magnetic intensity in the first and second position of the field, with three different magnetic M_n of 0.2, 1.6, and 2.8. **Error! Reference source not found.** and **Error! Reference source not found.** show the effect of changing the field number on particle deposition at positions 1 and 2. As can be seen, increasing the magnetic number increases deposition in the target area. Also, in field number 2.8, in the target regions 1 and 2 more particles have accumulated than other magnetic numbers. In Figure 5, at a lower magnetic number, the particles pass through the target point and enter the right iliac artery, but as the magnetic number increases, the magnetic particles carrying the drug accumulate in the target area and do not pass through that area and enter the right iliac artery. According to the results, particle deposition in the target area of the right iliac artery is much more than in the left iliac artery. It is demonstrated that a larger magnetic number can play an important role in the target area of the abdominal aorta. It is also estimated that the deposition efficiency (DE) of MNPs increases with increasing magnetic numbers. Comparing the three magnetic numbers applied, it can be stated that in the lower magnetic number, the particles follow the behavior of blood flow, and most of them pass through the area. Also, at higher magnitudes due to the strong magnetic force, which pulls most of the particles closer to the target area, the size of the CE, or the particles trapped in the target area, depends entirely on the strength of the magnetic field, since increasing the amount of external magnetic field will increase the magnetic force on the particle. Nevertheless, it should be noted that the increase in the magnetic field is severely limited. As the results of recent biomagnetic flow studies have shown, increasing the magnetic field changes the behavior of blood flow and the formation of the recirculation zone. Moreover, at magnetic number 0.2, the retention time of particles is much less than at magnetic number 2.8 in the target area. Besides, at low magnetic numbers, the particles pass through the target area and enter

the iliac artery. Therefore, regardless of the permissible magnetic field limit for the body, by applying higher magnetic field gradients, better effects on retention time will be observed while avoiding the risk of clogging or blockage of the vessel.

In **Error! Reference source not found.**, particle deposition was investigated for the magnetic number $M_n = 2$ at positions 1 and 2 for 0.82 seconds. As observed, 0.82 seconds with a magnetic number equal to the magnetic particles showed the same behavior for the two target areas. **Error! Reference source not found.** illustrates particle tracking using turbulent kinetic energy (TKE) for $M_n = 2$. Turbulent kinetic energy is calculated for a particle with a diameter of 1 nm and 100 nm. Turbulent kinetic energy for a particle with a maximum diameter of 1 nm is found in the target region, and turbulent kinetic energy for a particle with a maximum diameter of 100 nm is found in the aneurysm wall of the target area. It is also interesting to note that the effect of the external field on particles with a smaller diameter is less, and with increasing particle diameter and also due to the volumetric force, this effect increases. The purpose of this contour is to investigate the turbulence for diameters of 1 and 100 nm equal to the magnet number. As a result, nanoparticles with larger diameters and higher forces have more TKE than nanoparticles with smaller diameters.

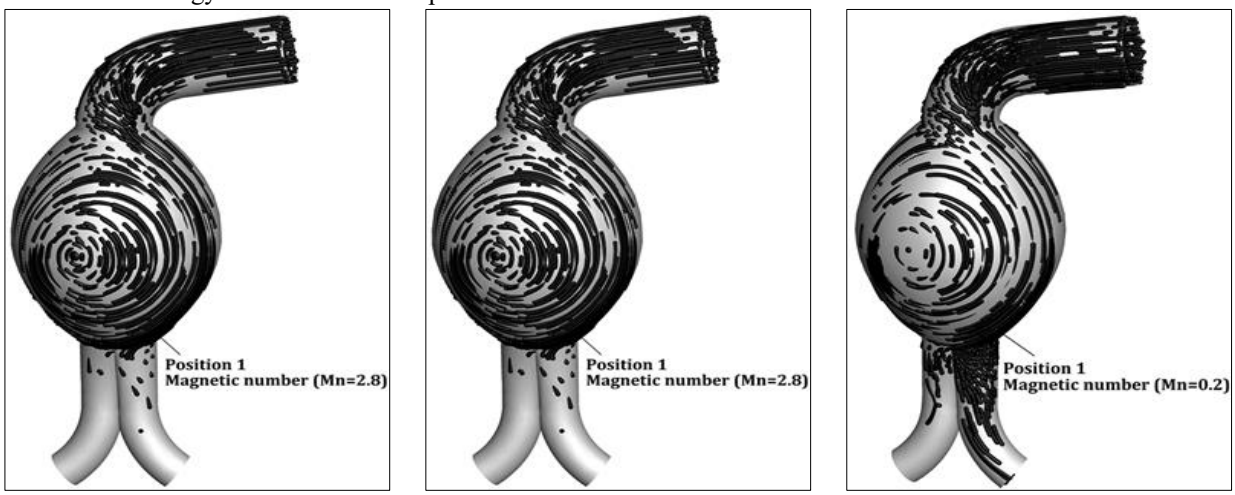

(a) (b) (c)

Figure 5. Effect of magnetic number on the particle transfer scheme for position 1 a) $M_n = 0.2$, b) $M_n = 1.6$, c) $M_n = 2.8$

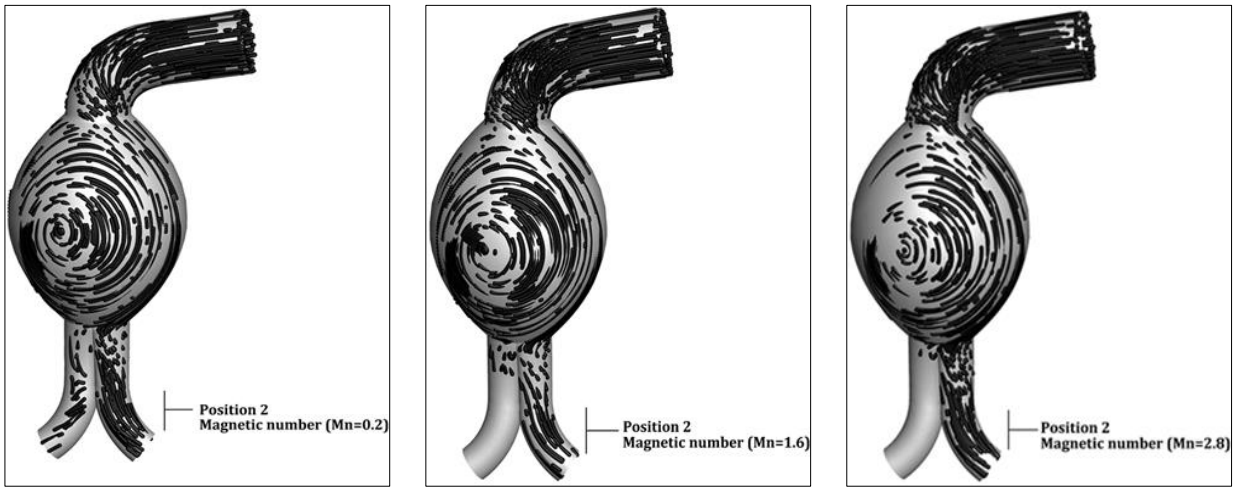

(a) (b) (c)

Figure 6. Effect of magnetic number on the particle transfer scheme for position 2 a) $M_n = 0.2$, b) $M_n = 1.6$, c) $M_n = 2.8$

In **Error! Reference source not found.**, particle deposition was investigated for the magnetic number $M_n = 2$ at positions 1 and 2 for 0.82 seconds. As observed, 0.82 seconds with a magnetic number equal to the magnetic particles showed the same behavior for the two target areas. **Error! Reference source not found.** illustrates particle tracking using turbulent kinetic energy (TKE) for $M_n = 2$. Turbulent kinetic energy is calculated for a particle with a diameter of 1 nm and 100 nm. Turbulent kinetic energy for a particle with a maximum diameter of 1 nm is found in the target region, and turbulent kinetic energy for a particle with a maximum diameter of 100 nm is found in the aneurysm wall of the target area. It is also interesting to note that the effect of the external field on particles with a smaller diameter is less, and with increasing particle diameter and also due to the volumetric force, this effect increases. The purpose of this contour is to investigate the turbulence for diameters of 1 and 100 nm equal to the magnet number. As a result, nanoparticles with larger diameters and higher

forces have more TKE than nanoparticles with smaller diameters.

Figure 9 illustrates the tracking of particles with turbulent kinetic energy (TKE), this time at a diameter of 60 nm and a time of 0.82 seconds but with different fields of 0.2, 1.6, and 2.8. As can be seen, the higher the magnetic number, the greater the amount of turbulent kinetic energy since increasing the magnetic number will increase the retention time of the particles and accelerate them. Therefore, in magnetic number 2.8, this perturbation is due to the increase of the gradient of the field and, consequently, the decrease of the diffusion effect relative to the volumetric force caused by the magnetic field. As a result, the accumulation of particles in the target region is higher than in the lower magnetic numbers.

Table 2 shows a general comparison of particle transport and deposition (TD) at two different target positions in 0.3 seconds for magnetic numbers 0.2, 1.6, and 2.8 and nanoparticles with diameters of 1, 15, 60, 100, and 600nm. According to Figure 4, the velocity peaks in 0.3 seconds, according to the deposition efficiency formula, and according to the table below, in 0.3 seconds, a larger magnetic number can play an important role in the particle deposition concentration in the target area of the abdominal aortic aneurysm.

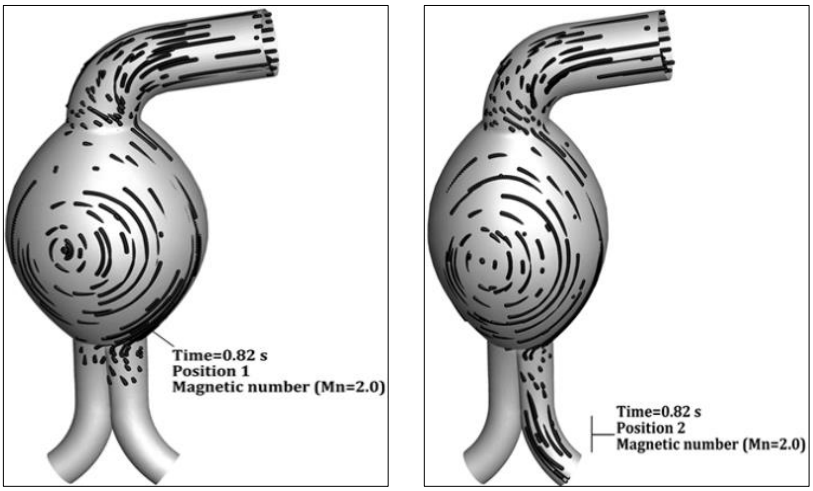

Figure 7. Particle deposition in the similar field and time (in second) in positions 1 and 2

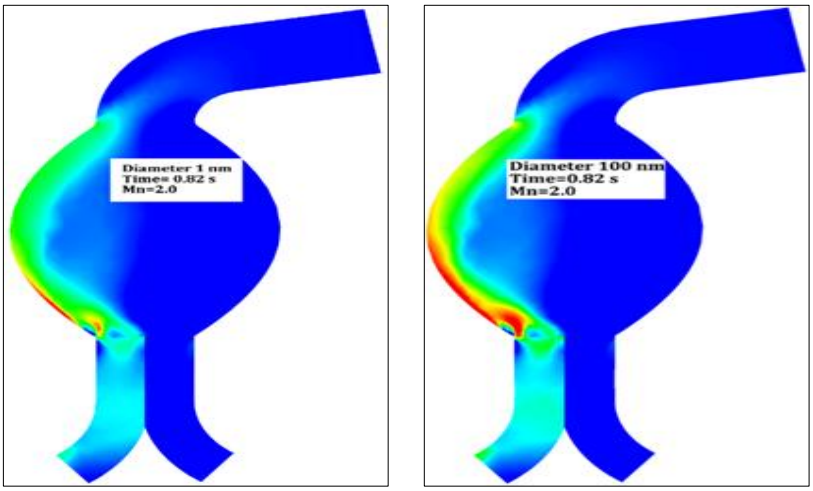

Figure 8. Particles Tracking with turbulent kinetic energy for magnetic number $M_n = 2$ and time =0.82 s, diameters 1 nm and 100nm

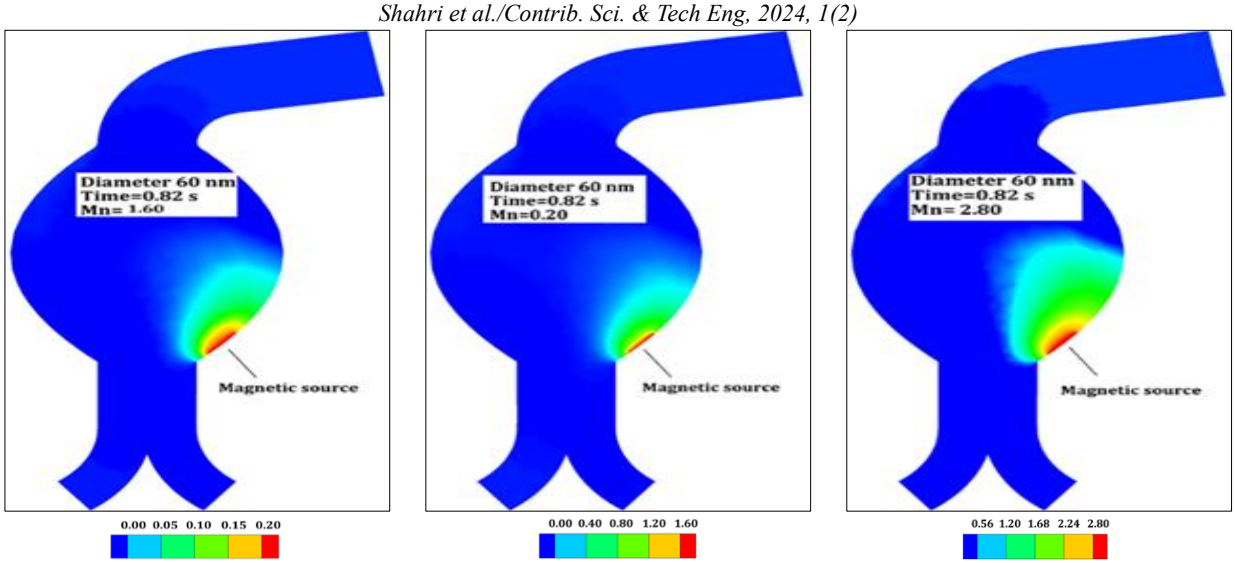

Figure 9. **Particles tracking with turbulent kinetic energy for particles with a diameter of 60 nm, time 0.82 s and magnetic numbers 0.2,1.6,2.8**

Table 2. **Comparison of TD in two different positions for magnetic numbers 0.2, 1.6, 2.8 in 0.3 seconds and particle diameters of 1, 15, 60, 100, and 600 nm**

Time =0.3 s	$M_n = 2.8$		$M_n = 1.6$		$M_n = 0.2$	
Diameter	**Position 1**	**Position 2**	**Position 1**	**Position 2**	**Position 1**	**Position 2**
1 nm	93.335%	48.333%	55.952%	26.555%	23.505%	18.885%
15 nm	88.425%	18.311%	64.521%	11.325%	26.312%	16.755%
60 nm	90.442%	31.200%	52.852%	12.425%	68.335%	19.415%
100 nm	96.244%	19.521%	67.424%	14.622%	39.742%	14.625%
600 nm	91.232%	21.537%	93.411%	21.227%	80.237%	21.007%

4. Conclusion

Considering that the drug transfer with Fe_3O_4 nanoparticles in aneurysm disease in the abdominal aorta and two left and right iliac vessels has not been studied and simulated in detail, in this study, it was comprehensively studied and simulated in Ansys-Fluent software. The present numerical results were validated with the analytical and numerical results of previous researchers and showed a good agreement. Computational fluid dynamics simulations for the severely ideal proximal neck of the 3D model AAA were performed based on the patient's hemodynamic parameters obtained from the experimental study. The main purpose of this study was to evaluate the effect of different magnetic numbers on the uptake of drug-carrying nanoparticles with different diameters in the proximal cervical vessels, aneurysm sac, and iliac arteries for abdominal aortic aneurysm. CFD tools were used to simulate and achieve this goal of the study. Changes in the magnetic number and diameter of nanoparticles through aneurysms and bifurcated arteries will be useful for understanding the intervention of cardiovascular disease.

An Angulated Neck of an Abdominal Aortic Aneurysm shows the deposition of magnetic nanoparticles (MNPs) in the target area of the human abdominal aneurysm. The existing numerical model also shows NPs in the range of 1≤nm ≤600 and magnetic numbers of 0.2, 1.6, and 2.8.

In this regard, a comprehensive validation has been performed, and the results are as follows:

- The effect of non-obvious forces such as weight and the effect of particle scattering due to magnetic field is expressed and recommended. In order to increase the retention time of particles in the vicinity of the damaged tissue, only high gradient fields should be used, and low gradient fields should be avoided because in low gradient fields, due to the relatively strong diffusion effect relative to the external force due to the field, the process of using magnetic nanoparticles may have an adverse effect on the outcome of drug therapy.
- The effects of particle diameter distribution in target positions 1 and 2 for 1, 15, 60, and 600 nm particles were investigated. Most particles deposit in the target position and on the side of the artery where the field is located (target area). In 0.3 seconds, the maximum number of depositions in the target position 1 is for 1, 15, 60, 100, and 600 nm diameters.
- The deposition scenario in the target position was investigated for three different magnetic numbers, i.e., 0.2, 1.6, and 2.8. The result shows that the total deposition concentration is higher in both magnetic field positions for a large magnetic number in 0.3 seconds.
- Nanoparticle deposition was investigated for two different magnetic source positions, namely position 1

and position 2. Most of the particles deposited on the wall are position 1 and position 2 (one of the iliac arteries depending on the position of the field), and the targeted magnetic particles are absorbed to the specific area of the aneurysm, which allows direct treatment of those specific cells. This system reduces damage to healthy cells in the body.

The results of the present study may be used to improve our understanding of the real drug delivery system in a targeted position of the proximal neck of the abdominal aortic aneurysm.

5. References

[1] Khonsary, S. (2017). Guyton and Hall: Textbook of Medical Physiology. Surgical Neurology International, 8(1), 275. doi:10.4103/sni.sni_327_17.

[2] Hong, L. S., Mohd Adib, M. A. H., Abdullah, M. S., & Hassan, R. (2020). Qualitative and quantitative comparison of hemodynamics between MRI measurement and CFD simulation on patient-specific cerebral aneurysm-A review. Journal of Advanced Research in Fluid Mechanics and Thermal Sciences, 68(2), 112–123. doi:10.37934/ARFMTS.68.2.112123.

[3] Tomaszewski, M., Sybilski, K., Baranowski, P., & Małachowski, J. (2020). Experimental and numerical flow analysis through arteries with stent using particle image velocimetry and computational fluid dynamics method. Biocybernetics and Biomedical Engineering, 40(2), 740–751. doi:10.1016/j.bbe.2020.02.010.

[4] Nowak, M. (2017). Identification and modelling of the pulsatile blood flow in section of elastic large blood vessel. Archiwum Instytutu Techniki Cieplnej, 3.

[5] Sarker, S., Chatzizisis, Y. S., & Terry, B. S. (2020). Computational optimization of a novel atraumatic catheter for local drug delivery in coronary atherosclerotic plaques. Medical Engineering and Physics, 79, 26–32. doi:10.1016/j.medengphy.2020.03.003.

[6] Zhang, X., Luo, M., Tan, P., Zheng, L., & Shu, C. (2020). Magnetic nanoparticle drug targeting to patient-specific atherosclerosis: effects of magnetic field intensity and configuration. Applied Mathematics and Mechanics (English Edition), 41(2), 349–360. doi:10.1007/s10483-020-2566-9.

[7] Sarker, S., Chatzizisis, Y. S., Kidambi, S., & Terry, B. S. (2018). Design and Development of a Novel Drug Delivery Catheter for Atherosclerosis. 2018 Design of Medical Devices Conference. doi:10.1115/dmd2018-6869.

[8] Li, J.-L., Liu, L.-N., & Gao, Y.-H. (2019). Research on Driving System of Hydraulic Robot Based on Ferrofluid. IOP Conference Series: Materials Science and Engineering, 688(3), 033077. doi:10.1088/1757-899x/688/3/033077.

[9] Shazri, S., & Idres, M. (2017). Numerical Investigation of Magnetic Nanoparticles Trajectories for Magnetic Drug Targeting. IOP Conference Series: Materials Science and Engineering, 184, 012061. doi:10.1088/1757-899x/184/1/012061.

[10] Jalali, S., Jalali, S., & Barati, E. (2024). Pulsatile blood flow simulations of magnetic drug targeting (MDT) for drug particles dispersion through stenosis asymmetric and symmetric vessels. Journal of Magnetism and Magnetic Materials, 590, 171649. doi:10.1016/j.jmmm.2023.171649.

[11] Park, M., Le, T. A., Hadadian, Y., & Yoon, J. (2022). Effects of major guidance parameters on aggregated magnetic particles during magnetic drug targeting. Journal of Magnetism and Magnetic Materials, 564, 170110. doi:10.1016/j.jmmm.2022.170110.

[12] Yew, Y. P., Shameli, K., Miyake, M., Ahmad Khairudin, N. B. B., Mohamad, S. E. B., Naiki, T., & Lee, K. X. (2020). Green biosynthesis of superparamagnetic magnetite Fe3O4 nanoparticles and biomedical applications in targeted anticancer drug delivery system: A review. Arabian Journal of Chemistry, 13(1), 2287–2308. doi:10.1016/j.arabjc.2018.04.013.

[13] Kim, D. H., Kim, D. W., Jang, J. Y., Lee, N., Ko, Y. J., Lee, S. M., Kim, H. J., Na, K., & Son, S. U. (2020). Fe3O4@Void@Microporous Organic Polymer-Based Multifunctional Drug Delivery Systems: Targeting, Imaging, and Magneto-Thermal Behaviors. ACS Applied Materials and Interfaces, 12(33), 37628–37636. doi:10.1021/acsami.0c12237.

[14] Hoshiar, A. K., Le, T. A., Amin, F. U., Kim, M. O., & Yoon, J. (2017). Studies of aggregated nanoparticles steering during magnetic-guided drug delivery in the blood vessels. Journal of Magnetism and Magnetic Materials, 427, 181–187. doi:10.1016/j.jmmm.2016.11.016.

[15] Lim, B. K., Tighe, E. C., & Kong, S. D. (2019). The use of magnetic targeting for drug delivery into cardiac myocytes. Journal of Magnetism and Magnetic Materials, 473, 21–25. doi:10.1016/j.jmmm.2018.09.118.

[16] Salem, S. F., & Tuchin, V. V. (2020). Numerical Simulation of Blood Flow in a Vessel by Using COMSOL Multiphysics® Software. Annual Research & Review in Biology, 35(9), 76–82. doi:10.9734/arrb/2020/v35i930274.

[17] Jafarzadeh, S., Nasiri Sadr, A., Kaffash, E., Goudarzi, S., Golab, E., & Karimipour, A. (2020). The Effect of Hematocrit and Nanoparticles Diameter on Hemodynamic Parameters and Drug Delivery in Abdominal Aortic Aneurysm with Consideration of Blood Pulsatile Flow. Computer Methods and Programs in Biomedicine, 195, 105545. doi:10.1016/j.cmpb.2020.105545.

[18] Sodagar, H., Shakiba, A., & Niazmand, H. (2020). Numerical investigation of drug delivery by using magnetic field in a 90-degree bent vessel: a 3D simulation. Biomechanics and Modeling in Mechanobiology, 19(6), 2255–2269. doi:10.1007/s10237-020-01337-0.

[19] Hobo, R., Kievit, J., Leurs, L. J., & Buth, J. (2007). Influence of severe infrarenal aortic neck angulation on complications at the proximal neck following endovascular AAA repair: A EUROSTAR study. Journal of Endovascular Therapy, 14(1), 1–11. doi:10.1583/06-1914.1.

[20] Akar, S., Abolfazli Esfahani, J., & Mousavi Shaegh, S. A. (2020). A numerical investigation on the Magnetophoretic-

guided stem cells delivery in a bend blood vessel. Journal of Magnetism and Magnetic Materials, 498, 166110. doi:10.1016/j.jmmm.2019.166110.

[21] Algabri, Y. A., Chatpun, S., & Taib, I. (2019). An investigation of pulsatile blood flow in an angulated neck of abdominal aortic aneurysm using computational fluid dynamics. Journal of Advanced Research in Fluid Mechanics and Thermal Sciences, 57(2), 265–274.

[22] Pourmehran, O., Gorji, T. B., & Gorji-Bandpy, M. (2016). Magnetic drug targeting through a realistic model of human tracheobronchial airways using computational fluid and particle dynamics. Biomechanics and Modeling in Mechanobiology, 15(5), 1355–1374. doi:10.1007/s10237-016-0768-3.

[23] Gori, F., & Boghi, A. (2011). Two new differential equations of turbulent dissipation rate and apparent viscosity for non-newtonian fluids. International Communications in Heat and Mass Transfer, 38(6), 696–703. doi:10.1016/j.icheatmasstransfer.2011.03.003.

[24] Pourmehran, O., Rahimi-Gorji, M., Gorji-Bandpy, M., & Gorji, T. B. (2015). Simulation of magnetic drug targeting through tracheobronchial airways in the presence of an external non-uniform magnetic field using Lagrangian magnetic particle tracking. Journal of Magnetism and Magnetic Materials, 393, 380–393. doi:10.1016/j.jmmm.2015.05.086.

[25] Ghosh, A., Islam, M. S., & Saha, S. C. (2020). Targeted drug delivery of magnetic nano-particle in the specific lung region. Computation, 8(1), 10. doi:10.3390/computation8010010.

[26] Bates, A. J., Schuh, A., Amine-Eddine, G., McConnell, K., Loew, W., Fleck, R. J., Woods, J. C., Dumoulin, C. L., & Amin, R. S. (2019). Assessing the relationship between movement and airflow in the upper airway using computational fluid dynamics with motion determined from magnetic resonance imaging. Clinical Biomechanics, 66, 88–96. doi:10.1016/j.clinbiomech.2017.10.011.

[27] Longest, P. W., & Xi, J. (2007). Computational investigation of particle inertia effects on submicron aerosol deposition in the respiratory tract. Journal of Aerosol Science, 38(1), 111–130. doi:10.1016/j.jaerosci.2006.09.007.

[28] Bose, S., & Banerjee, M. (2015). Magnetic particle capture for biomagnetic fluid flow in stenosed aortic bifurcation considering particle-fluid coupling. Journal of Magnetism and Magnetic Materials, 385, 32–46. doi:10.1016/j.jmmm.2015.02.060.